# Synthesis and Characterization of Tetrachlorodiarylethyne-Linked Porphyrin Dimers. Effects of Linker Architecture on Intradimer Electronic Communication

**Jon-Paul Strachan,[†] Steve Gentemann,[‡] Jyoti Seth,[§] William A. Kalsbeck,[§] Jonathan S. Lindsey,*[,†] Dewey Holten,*[,‡] and David F. Bocian*[,§]**

Departments of Chemistry, North Carolina State University, Raleigh, North Carolina 27695-8204, Washington University, St. Louis, Missouri 63130-4899, and University of California, Riverside, California 92521-0403

*Received July 31, 1997*

The effects of incorporating chloro groups at all ortho positions of a diphenylethyne linker that bridges the zinc and free base (Fb) components of a porphyrin dimer ($ZnFbB(Cl_4)$) have been investigated in detail via various static and time-resolved spectroscopic methods. The excited-state energy-transfer rate in $ZnFbB(Cl_4)$ ($(134\ ps)^{-1}$) is 5-fold slower than that in the corresponding dimer having an unsubstituted linker (ZnFbU, $(24\ ps)^{-1}$) but is only modestly slower than that in the dimer having *o*-methyl groups on the linker ($ZnFbB(CH_3)_4$, $(115\ ps)^{-1}$). The ground-state hole/electron-hopping rates in the oxidized bis-Zn analogues of all three dimers are much slower than the excited-state energy-transfer rates. There is no discernible difference between the hole/electron-hopping rates in the *o*-chloro- and *o*-methyl-substituted arrays. The similar ground- and excited-state dynamics observed for the *o*-chloro- and *o*-methyl-substituted arrays is attributed to the dominance of torsional constraints in mediating the extent of through-bond electronic communication. These constraints attenuate intradimer communication by restricting the rotation toward coplanarity of the phenyl rings of the linker and the porphyrin rings. Thus, the *o*-chloro groups on the linker decrease electronic communication via a steric, rather than purely electronic, mechanism.

## Introduction

Our groups have initiated a program in the design, synthesis, and characterization of multipigment arrays for studies of artificial photosynthesis and molecular photonics. Toward that end, we have investigated a variety of multiporphyrin arrays comprised of free base (Fb) porphyrins, metalloporphyrins, and other pigments that are joined by semirigid[1] diarylethyne linkers. These systems include a star-shaped pentameric array that serves as a light-harvesting device;[2] a linear array comprised of a boron dipyrromethene dye, three Zn porphyrins, and one Fb porphyrin that functions as a molecular photonic wire;[3] and a related array including a Mg porphyrin as a redox switch that serves as an optoelectronic gate.[4] These and related architectures are quite robust in terms of their convenient building-block syntheses, their stability and solubility, and their ultrafast and efficient energy-transfer properties. These favorable qualities indicate that the diphenylethyne-linker motif is ideal for incorporation into even larger and more complex arrays.

Toward optimizing our building-block strategy and exploring its full potential, we have investigated the factors that control electronic communication in three sets of diarylethyne-linked porphyrin dimers (Chart 1). An overarching finding is that both the singlet excited-state energy-transfer process in the neutral arrays and the ground-state hole/electron-hopping process in the oxidized complexes predominantly involve through-bond electronic communication mediated by the diarylethyne linker.[5−9] More specific findings of these studies are as follows.

**Chart 1.** Dimeric Arrays for Probing Energy Transfer

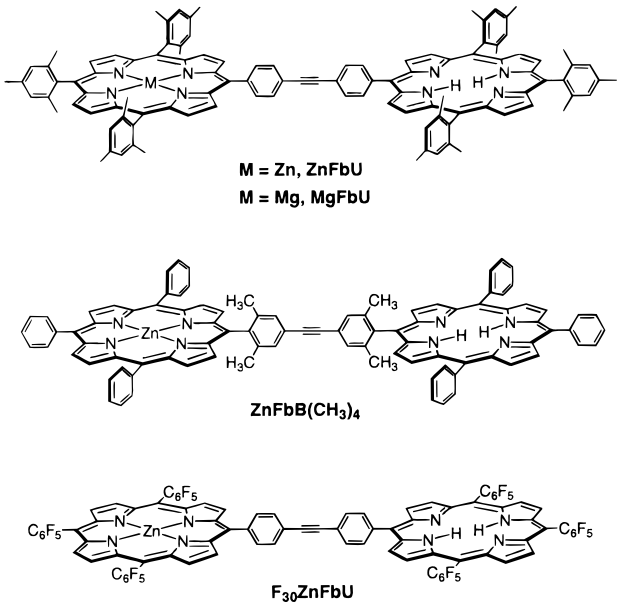


(1) The first series of dimers explored the effects of torsional constraints on the electronic communication. In particular, steric

[†] North Carolina State University.
[‡] Washington University.
[§] University of California.

(1) Bothner-By, A. A.; Dadok, J.; Johnson, T. E.; Lindsey, J. S. *J. Phys. Chem.* **1996**, *100*, 17551−17557.
(2) Prathapan, S.; Johnson, T. E.; Lindsey, J. S. *J. Am. Chem. Soc*. **1993**, *115*, 7519−7520.
(3) Wagner, R. W.; Lindsey, J. S. *J. Am. Chem. Soc.* **1994**, *116*, 9759−9760.
(4) Wagner, R. W.; Lindsey, J. S.; Seth, J.; Palaniappan, V.; Bocian, D. F. *J. Am. Chem. Soc.* **1996**, *118*, 3996−3997.
(5) Seth, J.; Palaniappan, V.; Johnson, T. E.; Prathapan, S.; Lindsey, J. S.; Bocian, D. F. *J. Am. Chem. Soc*. **1994**, *116*, 10578−10592.

S0020-1669(97)00967-1 CCC: $15.00 
Published on Web 03/03/1998

constraints that restrict the phenyl rings of the linker from rotating toward coplanarity with the porphyrin constituents result in a marked slowing of the energy-transfer rate. For example, the energy-transfer rate from the photoexcited Zn porphyrin (Zn*) to the Fb porphyrin is reduced from $\sim(24\ \text{ps})^{-1}$ in the unhindered dimer ZnFbU to $\sim(115\ \text{ps})^{-1}$ in the dimer having methyl groups at each of the ortho positions of the linker $ZnFbB(CH_3)_4$.[6,10] This difference derives predominantly from the sterically induced reduction in porphyrin-linker orbital overlap which attenuates through-bond electronic communication. This effect also modulates the ground-state hole/electron-hopping process in the oxidized bis-Zn analogues of the arrays $[Zn_2U]^+$ and $[Zn_2B(CH_3)_4]^+$. However, this latter process is much slower in both arrays ($(10-100\ \text{ns})^{-1}$) than the excited-state energy transfer.

(2) The second series of dimers explored the effects of metal substitution (Mg vs Zn) on the photodynamics of the torsionally unconstrained array.[8] The ZnFbU and MgFbU dimers exhibit comparable energy-transfer rates independent of solvent, although the longer intrinsic excited-state lifetime of the Mg porphyrin relative to that of the Zn porphyrin ($\sim$10 vs $\sim$2 ns) affords a slightly greater energy-transfer yield for the Mg-containing dimer. This difference, although slight for the isolated dimer, would be amplified in arrays having large numbers of energy-transfer steps. On the other hand, architectures having a Mg versus Zn porphyrin component suffer the disadvantages of slightly lower stability and enhanced electron transfer competing with energy migration.

(3) The third series of dimers revealed the novel effects of the nature and electron-density distribution of the highest occupied molecular orbital (HOMO) of the porphyrin constituents.[9] The energy-transfer rate in $F_{30}$ZnFbU ($(240\ \text{ps})^{-1}$), which contains pentafluorophenyl groups at all nonlinking meso carbons, is an order of magnitude slower than in ZnFbU ($(24\ \text{ps})^{-1}$), which contains mesityl groups at these positions. The $a_{1u}$ HOMOs of the porphyrins in the former dimer have nodes at the meso positions, including those to which the linker is appended. In contrast, the $a_{2u}$ HOMOs of the constituents of the latter array have substantial electron density at these positions. This reversal of orbital ordering, together with a redistribution in electron density accompanying incorporation of the electron-withdrawing fluorines, substantially diminishes electronic coupling via the linker and reduces the rates of both excited-state energy transfer and ground-state hole/electron hopping.

Our previous studies of diarylethyne-linked porphyrin arrays have afforded insights into the predominant mechanism of electronic communication and have revealed new strategies for optimizing these tetrapyrrole-based architectures for materials applications. Recently, one of our groups observed that *o*-chloro substituents on *meso*-phenyl rings directly interact with the p orbitals of the *meso*-carbon atoms of the porphyrin.[11] In order to examine whether this interaction could open a new conduit for enhanced electronic communication in diarylethyne-linked multiporphyrin arrays, we prepared ZnFb and bis-Zn dimers bearing chloro substituents at all ortho positions on the diphenylethyne linkers $ZnFbB(Cl_4)$ and $Zn_2B(Cl_4)$, as shown in Chart 2. We have examined these and related compounds by static spectroscopy (absorption, fluorescence, resonance Raman, electron paramagnetic resonance), time-resolved absorption spectroscopy, and electrochemical (cyclic and square-wave voltammetry, coulometry) techniques.

**Chart 2.** Structures of Dimeric Arrays and Porphyrin Building Blocks

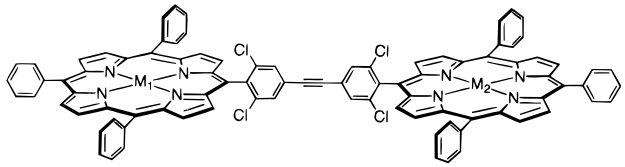

| $M_1$ | $M_2$ | cmpd |
|---|---|---|
| Zn | H, H | **$ZnFbB(Cl_4)$** |
| H, H | H, H | **$Fb_2B(Cl_4)$** |
| Zn | Zn | **$Zn_2B(Cl_4)$** |
| Cu | Cu | **$Cu_2B(Cl_4)$** |

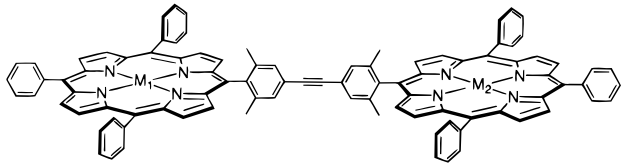

| $M_1$ | $M_2$ | cmpd |
|---|---|---|
| H, H | H, H | **$Fb_2B(CH_3)_4$** |
| Cu | Cu | **$Cu_2B(CH_3)_4$** |

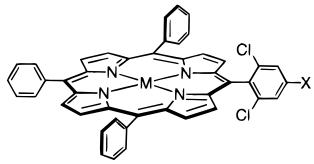

| M | X | cmpd |
|---|---|---|
| H, H | —I | **$FbIH(Cl_2)$** |
| Zn | −C≡C-TMS | **$ZnH(Cl_2)$** |
| H, H | −C≡C·H | **$FbH(Cl_2)'$** |
| Zn | −C≡C·H | **$ZnH(Cl_2)'$** |

## Experimental Section

**A. Synthetic Procedures. 1. General.** $^1$H NMR spectra (300 MHz, IBM FT-300), absorption spectra (HP 8453A, Cary 3), and fluorescence spectra (Spex FluoroMax) were collected routinely. Porphyrins were analyzed in neat form by laser desorption mass spectrometry (LD-MS)[12] or in a matrix (4-hydroxy-α-cyanocinnamic acid) (MALDI-TOF-MS)[12] using a Bruker Proflex II. Elemental analyses were obtained from Atlantic Micro Labs Inc. Pyrrole was distilled at atmospheric pressure from $CaH_2$. Commercial sources

(6) Hsiao, J.-S.; Krueger, B. P.; Wagner, R. W.; Delaney, J. K.; Mauzerall, D. C.; Fleming, G. R.; Lindsey, J. S.; Bocian, D. F.; Donohoe, R. J. *J. Am. Chem. Soc.* **1996**, *118*, 11181−11193.

(7) Seth, J.; Palaniappan, V.; Wagner, R. W.; Johnson, T. E.; Lindsey, J. S.; Bocian, D. F. *J. Am. Chem. Soc.* **1996**, *118*, 11194−11207.

(8) Li, F.; Gentemann, S.; Kalsbeck, W. A.; Seth, J.; Lindsey, J. S.; Holten, D.; Bocian, D. F. *J. Mater. Chem.* **1997**, *7*, 1245−1262.

(9) Strachan, J. P.; Gentemann, S.; Seth, J.; Kalsbeck, W. A.; Lindsey, J. S.; Holten, D.; Bocian, D. F. *J. Am. Chem. Soc.* **1997**, *119*, 11191−11201.

(10) The previous value for the energy-transfer rate for $ZnFbB(CH_3)_4$, $k_{trans} = (88\ \text{ps})^{-1}$, has been remeasured by transient absorption spectroscopy over a longer time frame. The revised value is $k_{trans} = (115\ \text{ps})^{-1}$, which is used throughout this paper.

(11) Kalsbeck, W. A.; Seth, J.; Bocian, D. F. *Inorg. Chem.* **1996**, *35*, 7935−7937.

(12) Fenyo, D.; Chait, B. T.; Johnson, T. E.; Lindsey, J. S. *J. Porphyrins Phthalocyanines* **1997**, *1*, 93−99.

provided (trimethylsilyl)acetylene (Janssen Chimica), 4-iodobenzaldehyde (Karl Industries Inc.), 2,6-dichlorobenzaldehyde (Aldrich), and all other reagents and starting materials (Aldrich). Melting points are uncorrected.

**2. Chromatography.** Preparative chromatography was performed using the "wet-flash" column technique[13] using flash silica (Baker) or alumina (Fisher A540, 80−200 mesh) and eluting solvents based on hexanes admixed with ether or $CH_2Cl_2$. Porphyrins were dissolved in $CH_2Cl_2$ and preadsorbed onto silica or alumina in a round-bottom flask. The solvent was removed on a rotary evaporator with gentle heating to avoid bumping. With the eluant level in the column a few centimeters above the adsorbent bed, the preadsorbed sample was added. Preparative scale size exclusion chromatography (SEC) was performed using BioRad Bio-Beads SX-1.[8,14] Analytical scale SEC was performed to assess the purity of the array-forming reactions and to monitor the preparative purification of the arrays. [8,14]

**3. Solvents.** $CH_2Cl_2$ (Fisher, reagent grade) was subjected to simple distillation from $K_2CO_3$. Dry $CH_2Cl_2$ (Fisher certified ACS), toluene (Fisher certified ACS), and triethylamine (Fluka puriss) were distilled from $CaH_2$. Other solvents were used as received.

**4. Synthetic Details. 2,6-Dichloro-4-iodoaniline (1).** To a solution of 2,6-dichloroaniline (9.05 g, 55.8 mmol) in 250 mL of dichloromethane and 100 mL of methanol were added benzyltrimethylammonium dichloroiodate ($BTMAICl_2$)[15] (22.50 g, 64.6 mmol) and calcium carbonate (7.23 g). The mixture was heated at reflux for 2 h under an argon atmosphere, during which time the solution gradually changed from yellow to orange. The solution was then stirred at room temperature overnight. Excess calcium carbonate was filtered, and the solvent was removed in vacuo. To the residue was added 5% w/v $NaHSO_4$ (25 mL), and the mixture was extracted with $CH_2Cl_2$ (4 × 100 mL). The organic layer was dried and filtered and the solvent removed in vacuo. Wet-flash column chromatography on silica (hexanes−ether (9:1)) gave a white solid (6.4 g, 40%). Mp: 96 °C from methanol (lit.[16] mp 96−97 °C from 30% alcohol). Anal. Found: ($M^+$), 286.8758. $C_6H_4Cl_2IN$ requires the following: ($M^+$), 286.8766. $^1$H NMR (300 MHz, $CDCl_3$): 4.48 (2 H, br, $NH_2$), 7.45 (2 H, s, Ar−H). $^{13}$C NMR (75 MHz, $CDCl_3$): 75.8 (quat, C−I), 120.2 (2 × quat, C−Cl), 135.7 (2 × CH), 140.0 (quat, C−$NH_2$). *m*/*z* (EI): 289 ($M^+$, 64%), 287 (100), 162 (24), 160 (39), 127 (30), 124 (41), 97 (10).

**2,6-Dichloro-4-iodobenzonitrile (3).** A hot mixture of equal amounts of concentrated $H_2SO_4$ and water (70 mL) was added to 2,6-dichloro-4-iodoaniline (**1**) (7.11 g, 24.7 mmol), and the resulting mixture was stirred for 10 min before cooling to 0 °C. On cooling a mass of the anilinium sulfate was obtained. Diazotization was effected at 0−5 °C with a solution of $NaNO_2$ (1.77 g, 25.6 mmol) in 25 mL of water.[17] The solution was filtered and diluted with 150 g of ice. A solution of $NaBF_4$ (32.4 g, 295 mmol) dissolved in the minimum amount of $H_2O$ was then added to the diazonium solution. The precipitate was filtered and washed with 25 mL of a saturated $NaBF_4$ solution, 10 mL of methanol and 25 mL of ether. The resultant yellow solid was dried in vacuo. The tetrafluoroborate diazonium salt (**2**) dissolved in ∼400 mL of $H_2O$ was added dropwise at 0 °C with vigorous stirring to a cuprous cyanide mixture. [Cuprous cyanide (2.32 g, 25.9 mmol) was suspended in 120 mL of water. Aqueous sodium cyanide (15 mL, 3.2 g, 65.3 mmol) was added and the mixture stirred at room temperature until the cuprous cyanide dissolved.] When the addition was complete, the mixture was stirred at 0 °C for 1 h and at room temperature for 1 h. $CH_2Cl_2$ (3 × 100 mL) was added, and the organic layer was separated, washed with 50 mL of water, and dried ($MgSO_4$), and the solvent was removed in vacuo. Gravity column chromatography on silica (hexanes−ethyl acetate (9:1)) gave an orange solid which was sublimed at 90 °C/0.1 mmHg to give a white solid (1.77 g, 24%). Mp 117−119 °C. Anal. Found: C, 28.3; H, 0.8; N, 4.7; Cl, 23.8; I, 42.6; ($M^+$), 296.8604. $C_7H_2Cl_2IN$ requires the following: C, 28.2; H, 0.7; N, 4.7; Cl, 23.8; I, 42.6; ($M^+$), 296.8609. $^1$H NMR (300 MHz, $CDCl_3$): 7.82 (2 H, s, Ar−H). $^{13}$C NMR (75 MHz, $CDCl_3$): 99.2 (quat, C−I), 112.9 (quat, *C−CN), 114.0 (quat, CN), 137.0 (2 × CH), 138.4 (2 × quat, C−Cl). *m*/*z* (EI): 299 ($M^+$, 60%), 297 (100), 172 (55), 170 (100), 134 (50), 127 (15), 99 (40). IR $\nu_{max}$(Nujol)/cm$^{-1}$: 2234 (CN).

**2,6-Dichloro-4-iodobenzaldehyde (4).** A sample of 2,6-dichloro-4-iodobenzonitrile (**3**) (1.5 g, 5.04 mmol) was dissolved in 5 mL of dry $CH_2Cl_2$ (distilled from $CaH_2$), and the solution was cooled to 0 °C. A 6.04 mL solution of DIBAL-H (6.04 mmol, 1 M in $CH_2Cl_2$) was added dropwise. After the addition was complete, the reaction mixture was allowed to warm to room temperature and was stirred for 30 min. The reaction mixture was then poured into a conical flask containing 20 g of ice and 20 mL of 6 N HCl. After 1 h of stirring, the aqueous layer was separated and extracted with $CH_2Cl_2$ (2 × 25 mL). The organic layers were combined, washed with 5% w/v $NaHCO_3$ (20 mL) and brine (20 mL), and dried ($MgSO_4$), and the solvent was removed in vacuo. Gravity column chromatography on silica (hexanes−ether (9:1)) gave a pale orange solid which was sublimed at 80 °C/0.1 mmHg, affording a white solid (1.36 g, 90%). Mp: 86−87 °C. Anal. Found: C, 28.0; H, 1.0; Cl, 23.5; I, 42.1; ($M^+$), 299.8602. $C_7H_3Cl_2IO$ requires the following: C, 27.9; H, 1.0; Cl, 23.6; I, 42.2; ($M^+$), 299.8606. $^1$H NMR (300 MHz, $CDCl_3$): 7.77 (2 H, s, Ar−H), 10.41 (1 H, s, CHO). $^{13}$C NMR (75 MHz, $CDCl_3$): 99.0 (quat, C−I), 129.8 (quat, *C−CHO), 137.1 (2 × quat, C−Cl), 138.3 (2 × CH), 187.8 (CHO) *m*/*z* (EI): 301 ($M^+$, 40%), 300 (50), 299 (100), 272 (10), 172 (25), 109 (60), 74 (75). IR $\nu_{max}$(Nujol)/cm$^{-1}$: 1684 (CHO).

**2,6-Dichloro-4-[2-(trimethylsilyl)ethynyl]benzaldehyde (5).** Samples of 2,6-dichloro-4-iodobenzaldehyde (**4**) (0.8 g, 2.66 mmol) and $AsPh_3$ (195 mg, 0.64 mmol) were dissolved in 20 mL of $Et_3N$ at room temperature. The solution was deaerated with argon for 15 min. (Trimethylsilyl)acetylene (0.45 mL, 3.18 mmol, 1.2 molar equiv) was added to the solution via syringe. $Pd_2(dba)_3$ (72 mg, 79 $\mu$mol) was added, and the reaction vessel was capped and placed in an oil bath at 35 °C. The reaction mixture was stirred at 35 °C under an argon atmosphere until GC-MS analyses showed the absence of starting material (48 h); an additional sample of (trimethylsilyl)acetylene (0.2 mL) was added after 24 h. The solvents were removed in vacuo and wet-flash column chromatography on silica (hexanes) gave an off-white solid, which was sublimed at 70 °C/0.1 mmHg (0.56 g, 78%). Mp 58 °C. Anal. Found: C, 53.0; H, 4.4; Cl, 26.0; ($M^+$), 270.0031. $C_{12}H_{12}Cl_2OSi$ requires the following: C, 53.4; H, 4.5; Cl, 25.8; ($M^+$), 270.0034). $^1$H NMR (300 MHz, $CDCl_3$): 0.25 (9 H, s, $Si(CH_3)_3$), 7.44 (2 H, s, Ar−H), 10.44 (1 H, s, CHO). $^{13}$C NMR (75 MHz, $CDCl_3$): −0.4 (3 × $CH_3$, $Si(CH_3)_3$), 100.9 (quat, *C−ethyne), 101.5 (quat), 129.2 (quat, *C−CHO), 129.7 (quat), 132.6 (2 × CH), 136.7 (2 × quat, C−Cl), 188.0 (CHO). *m*/*z* (EI): 272 ($M^+$, 40%), 270 (75), 255 (100), 127 (20), 113 (10). IR $\nu_{max}$(Nujol)/cm$^{-1}$: 1710 (CHO).

**5,10,15-Triphenyl-20-(2,6-dichloro-4-iodophenyl)porphyrin (FbI-H($Cl_2$)).** Pyrrole (92 $\mu$L, 1.33 mmol), benzaldehyde (101.5 $\mu$L, 0.997 mmol), and 2,6-dichloro-4-iodobenzaldehyde (**5**) (0.1 g, 0.332 mmol) were dissolved in 135 mL of $CH_2Cl_2$ under an argon atmosphere. After 10 min, $BF_3{\cdot}O(Et)_2$ (0.2 mL of a 2.65 M stock solution, 0.4 mmol) was added via syringe with vigorous stirring. After addition was complete, the reaction mixture was stirred for 1 h at room temperature. DDQ (0.30 g, 1.33 mmol) was added, and after 1 h of stirring at room temperature, the solvent was removed in vacuo. Wet-flash column chromatography on silica (hexanes−$CH_2Cl_2$ (4:1)) gave a mixture of porphyrins. Wet-flash column chromatography on alumina (hexanes−$CH_2Cl_2$ (4:1)), gave a mixture of two porphyrins. These were separated on alumina (hexanes−$CH_2Cl_2$ (4:1)) affording a purple solid (50 mg, 18.4%). $^1$H NMR (300 MHz, $CDCl_3$): −2.71 (2 H, s, NH), 7.76 (9 H, m, Ar−H), 8.15 (2 H, s, Ar−H), 8.20 (6 H, m, Ar−H), 8.65 (2 H, d, $J$ = 4.8 Hz, $\beta$-pyrrole), 8.82 (4 H, s, $\beta$-pyrrole), 8.88 (2 H, d, $J$ = 4.8 Hz, $\beta$-pyrrole). MALDI-TOF-MS $C_{44}H_{27}Cl_2IN_4$: calcd av mass, 808.1; obsd *m*/*z*, 809.0. $\lambda_{abs}$(toluene)/nm: 421, 514, 547, 590, 646.

**Zinc(II) 5,10,15-Triphenyl-20-[2,6-dichloro-4-{2-(trimethylsilyl)-ethynyl}phenyl]porphyrin (ZnH($Cl_2$)).** Pyrrole (349 $\mu$L, 5.05 mmol), benzaldehyde (384 $\mu$L, 3.78 mmol), and 2,6-dichloro-4-[2-(trimethyl-

(13) Still, W. C.; Kahn, M.; Mitra, A. *J. Org. Chem.* **1978**, *43*, 2923.
(14) (a) Wagner, R. W.; Johnson, T. E.; Lindsey, J. S. *J. Am. Chem. Soc.* **1996**, *118*, 11166−11180. (b) Nishino, N.; Wagner, R. W.; Lindsey, J. S. *J. Org. Chem.* **1996**, *61*, 7534−7544.
(15) Kajigaeshi, S.; Kakinami, T.; Yamasaki, H.; Fujisaki, S.; Okamoto, T. *Bull. Chem. Soc. Jpn.* **1988**, *61*, 600−602.
(16) Kutepov, D. F.; Kholkhlov, D. N.; Tuzhilkina, V. L. *Zh. Obshch. Khim.* **1960**, *30*, 2470.
(17) Lamm, B.; Andersson, B. *Ark. Kemi* **1966**, *25*, 367.

silyl)ethynyl]benzaldehyde (**5**) (0.34 g, 1.25 mmol) were dissolved in 515 mL of $CH_2Cl_2$ under an argon atmosphere. After 10 min, $BF_3{\cdot}O(Et)_2$ (0.76 mL of a 2.65 M stock solution, 1.51 mmol) was added via syringe with vigorous stirring. After addition was complete, the reaction mixture was stirred for 1 h at room temperature. DDQ (1.15 g, 5.05 mmol) was added and, after 1 h of stirring at room temperature, the solvent was removed in vacuo. The crude reaction mixture was passed through a short silica column (hexanes−$CH_2Cl_2$ (3:2)). The mixture of porphyrins was dissolved in 25 mL of $CH_2Cl_2$, and a solution of $Zn(OAc)_2{\cdot}2H_2O$ (445 mg, 2.03 mmol) in 5 mL of methanol was added. The reaction mixture was stirred under an argon atmosphere at room temperature overnight. The solvents were removed in vacuo, and wet-flash column chromatography on silica (hexanes−$CH_2Cl_2$ (4:1)) afforded a pink/purple solid (190 mg, 18.0%). $^1$H NMR (300 MHz, $CDCl_3$): 0.36 (9 H, s, $Si(CH_3)_3$), 7.75 (9 H, m, Ar−H), 7.90 (2 H, s, Ar−H), 8.21 (6 H, m, Ar−H), 8.74 (2 H, d, $J$ = 4.7 Hz, $\beta$-pyrrole), 8.92 (4 H, s, $\beta$-pyrrole), 8.95 (2 H, d, $J$ = 4.7 Hz, $\beta$-pyrrole). MALDI-TOF-MS $C_{49}H_{34}Cl_2N_4SiZn$: calcd av mass, 840.1, obsd $m/z$, 841.1. $\lambda_{abs}$(toluene)/nm: 423, 558.

**Zinc(II) 5,10,15-Triphenyl-20-[2,6-dichloro-4-ethynylphenyl]porphyrin (ZnH(Cl$_2$)′).** A sample of $ZnH(Cl_2)$ (145 mg, 0.17 mmol) was dissolved in 10 mL of freshly distilled THF. Tetrabutylammonium fluoride on silica (345 mg, 1.0−1.5 mmol F/g resin) was added and the reaction mixture stirred under argon for 30 min. The solvent was removed in vacuo, and wet-flash column chromatography on silica (hexanes−$CH_2Cl_2$ (7:3)) afforded a pink/purple solid (118 mg, 90%). $^1$H NMR (300 MHz, $CDCl_3$): 3.37 (1 H, s, CH), 7.75 (9 H, m, Ar−H), 7.92 (2 H, s, Ar−H), 8.21 (6 H, m, Ar−H), 8.74 (2 H, d, $J$ = 4.7 Hz, $\beta$-pyrrole), 8.92 (4 H, s, $\beta$-pyrrole), 8.96 (2 H, d, $J$ 4.7 = Hz, $\beta$-pyrrole). LD-MS $C_{46}H_{26}Cl_2N_4Zn$: calcd av mass, 768.0; obsd $m/z$, 767.4. $\lambda_{abs}$(toluene)/nm: 424, 550.

**5,10,15-Triphenyl-20-[2,6-dichloro-4-ethynylphenyl]porphyrin (FbH(Cl$_2$)′).** A sample of zinc porphyrin $ZnH(Cl_2)'$ (15 mg, 19.5 $\mu$mol) was dissolved in 5 mL of $CH_2Cl_2$ and treated with TFA (12 $\mu$L, 156 $\mu$mol). The demetalation was complete after 10 min, as evidenced by TLC. Triethylamine (33 $\mu$L, 234 $\mu$mol) was added and the reaction mixture stirred for another 10 min. The solution was washed with 10% w/v $NaHCO_3$ (5 mL) and dried ($Na_2SO_4$) and the solvent removed in vacuo. Wet-flash column chromatography on silica (hexanes−$CH_2Cl_2$ (4:1)) afforded a purple solid (13.7 mg, 100%). $^1$H NMR (300 MHz, $CDCl_3$): −2.70 (2 H, s, NH), 3.38 (1 H, s, CH), 7.75 (9 H, m, Ar−H), 7.92 (2 H, s, Ar−H), 8.25 (6 H, m, Ar−H), 8.65 (2 H, d, $J$ 4.7 Hz, $\beta$-pyrrole), 8.82 (4 H, s, $\beta$-pyrrole), 8.88 (2 H, d, $J$ = 4.7 Hz, $\beta$-pyrrole). LD-MS $C_{46}H_{28}Cl_2N_4$: calcd av mass, 706.2; obsd $m/z$, 706.7. $\lambda_{abs}$(toluene)/nm: 420, 514, 546, 590, 646.

**5,10,15-Triphenyl-20-[4-iodo-2,6-dimethylphenyl[porphyrin (FbIH(CH$_3$)$_2$).** See ref 14a.

**5,10,15-Triphenyl-20-[4-ethynyl-2,6-dimethylphenyl]porphyrin (FbH(CH$_3$)$_2$′).** See ref 14a.

**Procedure for Performing Pd-Coupling Reactions: 4-[Zinc(II) 10,15,20-triphenyl-5-porphinyl]-4′-[10,15,20-triphenyl-5-porphinyl]-3,5,3′,5′-tetrachlorodiphenylethyne (ZnFbB(Cl$_4$)).** 5,10,15-Triphenyl-20-(2,6-dichloro-4-iodophenyl)porphyrin ($FbIH(Cl_2)$) (50 mg, 61.7 $\mu$mol) and zinc(II) 5,10,15-triphenyl-20-[2,6-dichloro-4-ethynylphenyl]-porphyrin ($ZnH(Cl_2)'$) (55 mg, 64.9 $\mu$mol) were added to a 50 mL round-bottom flask containing 20.8 mL of toluene and 4.2 mL of $Et_3N$. The flask was fitted with a reflux condenser, and a glass pipet was inserted through the top. A stream of argon was passed through the pipet into the solution for 15 min. The pipet was raised and the reaction vessel purged for a further 10 min. $AsPh_3$ (19.0 mg, 62.1 $\mu$mol) and $Pd_2(dba)_3$ (8.3 mg, 9.1 $\mu$mol) were then added and the reaction vessel was placed in an oil bath at 35 °C. The reaction mixture was stirred at 35 °C until SEC analyses showed the absence of starting material (2 h). The solvents were removed in vacuo, and wet-flash column chromatography on silica (hexanes−$CH_2Cl_2$ (4:1)) removed all traces of the $AsPh_3$. The eluting solvent was then changed (hexanes−$CH_2Cl_2$ (1:1)) to elute monomeric porphyrins, desired dimer, and higher molecular weight material (HMWM). The mixture of porphyrins was concentrated to dryness, dissolved in the minimum amount of THF, loaded onto the top of a preparative SEC column (2.5 cm × 45 cm) (Bio-Beads SX-1 poured in THF), and eluted with THF. The desired dimer eluted as the second band, contaminated with some HMWM and monomer. The dimer was reloaded onto the SEC column and eluted with THF. The desired fraction was concentrated to dryness and passed through a silica column (hexanes−$CH_2Cl_2$ (3:2)) to give the title compound (free of HMWM and monomer by analytical SEC) as a purple solid (67 mg, 75%) $^1$H NMR (300 MHz, $CDCl_3$): −2.65 (2 H, s, NH), 7.78 (18 H, m, Ar−H), 8.11 (4 H, m, Ar−H), 8.24 (12 H, m, Ar−H), 8.75 (4 H, d, $J$ = 4.7 Hz, $\beta$-pyrrole), 8.84 (4 H, s, $\beta$-pyrrole), 8.95 (4 H, s, $\beta$-pyrrole), 9.02 (4 H, d, $J$ = 4.7 Hz, $\beta$-pyrrole); MALDI-TOF-MS $C_{90}H_{52}Cl_4N_8Zn$: calcd av mass, 1448.2, obsd $m/z$, 1447.1. $\lambda_{abs}$(toluene)/nm: 426, 515, 550, 591, 646.

**4,4′-Bis[10,15,20-triphenyl-5-porphinyl]-3,5,3′,5′-tetramethyldiphenylethyne (Fb$_2$B(CH$_3$)$_4$).** Samples of $FbIH(CH_3)_2$ (33 mg, 43 $\mu$mol) and $FbH(CH_3)_2'$ (30 mg, 45 $\mu$mol) were coupled following the standard procedure (2 h), affording the title compound (free of HMWM and monomer by analytical SEC) as a purple solid (39 mg, 70%). $^1$H NMR (300 MHz, $CDCl_3$): −2.66 (4 H, s, NH), 1.95 (12 H, s, $CH_3$), 7.77 (18 H, m, Ar−H), 7.82 (4 H, s, Ar−H), 8.26 (12 H, m, Ar−H), 8.75 (4 H, d, $J$ = 4.7 Hz, $\beta$-pyrrole), 8.85 (8 H, s, $\beta$-pyrrole), 8.87 (4 H, d, $J$ = 4.7 Hz, $\beta$-pyrrole), LD-MS $C_{94}H_{66}N_8$ calcd av mass, 1306.5; obsd $m/z$, 1305.6. $\lambda_{abs}$(toluene)/nm: 422, 513, 547, 592, 646.

**4,4′-Bis[zinc(II) 10,15,20-triphenyl-5-porphinyl]-3,5,3′,5′-tetrachlorodiphenylethyne Zn$_2$B(Cl$_4$).** A sample of $ZnFbB(Cl_4)$ (14 mg, 9.64 $\mu$mol) was dissolved in 5 mL of $CH_2Cl_2$, and then a methanolic solution of $Zn(OAc)_2{\cdot}2H_2O$ (5 mg, 22.8 $\mu$mol, 500 $\mu$L of methanol) was added. The reaction mixture was stirred overnight at room temperature and was checked prior to workup by TLC (hexanes−$CH_2Cl_2$ (1:1)). The solvents were removed in vacuo, and wet-flash column chromatography on silica (hexanes−$CH_2Cl_2$ (3:2)) afforded a pink/purple solid (14.6 mg, 100%). $^1$H NMR (300 MHz, $CDCl_3$): 7.78 (18 H, m, Ar−H), 8.11 (4 H, s, Ar−H), 8.24 (12 H, m, Ar−H), 8.84 (4 H, d, $J$ = 4.7 Hz, $\beta$-pyrrole), 8.94 (8 H, s, $\beta$-pyrrole), 9.02 (4 H, d, $J$ = 4.7 Hz, $\beta$-pyrrole). LD-MS $C_{90}H_{50}Cl_4N_8Zn_2$: calc av mass, 1510.2; obsd $m/z$, 1510.2. $\lambda_{abs}$(toluene)/nm: 427, 550.

**4,4′-Bis[cupric(II) 10,15,20-triphenyl-5-porphinyl]-3,5,3′,5′-tetrachlorodiphenylethyne (Cu$_2$B(Cl$_4$)).** A sample of $ZnFbB(Cl_4)$ (10 mg, 6.9 $\mu$mol) was dissolved in 5 mL of $CH_2Cl_2$ and treated with TFA (5 $\mu$L, 65 $\mu$mol). The demetalation was complete after 10 min, as evidenced by TLC. $Et_3N$ (14 $\mu$L, 98 $\mu$mol) was added and the reaction mixture stirred for another 10 min. The solution was washed with 10% w/v $NaHCO_3$ (5 mL) and dried ($Na_2SO_4$) and the solvent removed in vacuo. Wet-flash column chromatography on silica (hexanes−$CH_2Cl_2$ (4:1)) afforded $Fb_2B(Cl_4)$ as a purple solid. A sample of $Fb_2B(Cl_4)$ (9.5 mg, 6.9 $\mu$mol) was dissolved in 5 mL of $CH_2Cl_2$, and then a methanolic solution of $Cu(OAc)_2{\cdot}2H_2O$ (28 mg, 138 $\mu$mol, 500 $\mu$L of methanol) was added. The reaction mixture was stirred overnight at room temperature and was checked prior to work-up by TLC (hexanes−$CH_2Cl_2$ (2:1)). The solvents were removed in vacuo, and wet-flash column chromatography on silica (hexanes−$CH_2Cl_2$ (4:1)) afforded a pink/purple solid (10 mg, 99%). LD-MS $C_{90}H_{50}Cl_4Cu_2N_8$: calcd av mass, 1508.2; obsd $m/z$, 1509.5. $\lambda_{abs}$(toluene)/nm: 421, 542.

**4,4′-Bis[cupric(II) 10,15,20-triphenyl-5-porphinyl]-3,5,3′,5′-tetramethyldiphenylethyne (Cu$_2$B(CH$_3$)$_4$).** A sample of $Fb_2B(CH_3)_4$ (15 mg, 11.4 $\mu$mol) was dissolved in 5 mL of $CH_2Cl_2$, and then a methanolic solution of $Cu(OAc)_2{\cdot}2H_2O$ (46 mg, 230 $\mu$mol, 500 $\mu$L of methanol) was added. The reaction mixture was stirred overnight at room temperature and was checked prior to work-up by TLC (hexanes−$CH_2Cl_2$ (2:1)). The solvents were removed in vacuo, and wet-flash column chromatography on silica (hexanes−$CH_2Cl_2$ (4:1)) afforded a pink/purple solid (16 mg, 99%). LD-MS $C_{94}H_{62}Cu_2N_8$: calcd av mass, 1428.4; obsd $m/z$, 1426.9. $\lambda_{abs}$(toluene)/nm: 420, 540.

**B. Physical Methods.** The static and time-resolved absorption and fluorescence studies were performed on samples prepared in toluene or DMSO at room temperature. Toluene (EMI, Omnisolve) was distilled from sodium; DMSO (Mallinckrodt) was used without further purification. The samples for time-resolved fluorescence measurements were degassed by several freeze−pump−thaw cycles on a high-vacuum line. The samples for static fluorescence and time-resolved absorption measurements were not degassed. The RR, electrochemical, and EPR studies were performed on samples prepared in $CH_2Cl_2$. $CH_2Cl_2$ (Aldrich, HPLC Grade) was purified by vacuum distillation from $P_2O_5$

followed by another distillation from $CaH_2$. For the electrochemical studies, tetrabutylammonium hexafluorophosphate (TBAH; Aldrich, recrystallized three times from methanol and dried under vacuum at 110 °C) was used as the supporting electrolyte. The solvents were degassed thoroughly by several freeze−pump−thaw cycles prior to use.

**1. Static Absorption and Fluorescence Spectroscopy.** Static absorption and emission measurements were performed as described previously.[6,8,9] The extinction coefficients ($M^{-1}cm^{-1}$) for the porphyrin monomers in toluene at room temperature at the Soret band and Q-region maximum (510 nm for Fb complexes or 550 nm for the Zn complexes) were determined to be as follows: $ZnH(Cl_2)$, 325 000 and 18 000; $ZnH(Cl_2)'$, 349 000 and 21 000; $FbH(Cl_2)'$, 387 000 and 19 500; $FbIH(Cl_2)$, 211 000 and 11 000.

**2. Time-Resolved Absorption and Fluorescence Spectroscopy.** Transient absorption data were acquired as described elsewhere.[8,9,18] Samples were excited with 0.2-ps, 582-nm, 100-$\mu$J flashes at 10 Hz and had a concentration of ∼0.2 mM for measurements between 450 and 560 nm and of ∼0.6 mM for measurements to the red of 595 nm. Fluorescence lifetimes were acquired as described previously[8,9] on an apparatus having a time response of ∼0.5 ns, using samples having a concentration of ∼0.2 mM.

**3. RR Spectroscopy.** The RR spectra were acquired as described previously,[9] on samples that typically had a concentration of 0.05 mM (B-state excitation) or 0.5 mM (Q-state excitation). The laser power at the sample was typically 3 mW, and the spectral resolution was ∼3 $cm^{-1}$ at a Raman shift of 1600 $cm^{-1}$.

**4. Electrochemistry.** The oxidized complexes were prepared and manipulated in a glovebox as described previously.[9] The integrity of the samples was checked by cyclic voltammetry after each successive oxidation. In all cases, the cyclic voltammograms were reproducible upon repeated scans and exhibited no scan rate dependence in the 20−100 mV/s range. Studies were performed immediately after oxidation and transfer of the samples to an optical cuvette (absorption) or quartz capillary (EPR).

**5. EPR Spectroscopy.** The EPR spectra were recorded as described previously.[9] The sample concentration for all the experiments was typically 0.05 mM. The microwave power and magnetic field modulation amplitude were typically 5.7 mW and 0.32 G, respectively.

## Results and Discussion

**A. Synthesis of the Porphyrin Building Blocks and Arrays.** The synthesis of the arrays relies on a modular building-block approach that involves repetitive use of a small set of chemical reactions.[14,19,20] The arrays are constructed by joining free base or metalloporphyrins that bear iodo or ethyne groups. The porphyrins in turn are constructed from pyrrole and the appropriate benzaldehyde using a room-temperature synthetic method.[21,22] Incorporating the desired porphyrin substituents in the aldehyde precursor minimizes synthetic manipulation of the porphyrins.

**1. Aldehydes.** The 2,6-dichloro-substituted benzaldehydes required for the synthesis of arrays bearing chloro substituents in the linker were prepared according to Scheme 1. The reaction of 2,6-dichloroaniline with $BTMAICl_2$[15] in $CH_2Cl_2$-MeOH at reflux for 2 h gave the 2,6-dichloro-4-iodoaniline (**1**) in 40% yield. The diazotization reaction failed when concentrated hydrochloric acid and sodium nitrite were used, which we attribute to the formation of byproducts resulting from halogen−halogen exchange.[23] To avoid this problem the stable tetrafluoroborate diazonium salt (**2**) was synthesized.[17] Compound **1** was added to hot sulfuric acid to form the anilinium sulfate and then reacted with sodium nitrite to give the diazonium ion, which was isolated as the salt upon addition of sodium tetrafluoroborate. Treatment of the diazonium salt with a cuprous cyanide mixture gave the 4-iodobenzonitrile (**3**) in 24% yield. The major byproducts as seen by GC-MS were 2,4,6-trichloroaniline, dichlorodiiodobenzene, and 3,5-dichloroiodobenzene. The benzonitrile **3** was reduced using 1.1 molar equiv of DIBAL-H, affording aldehyde **4** in 80% yield. Treatment of 2,6-dichloro-4-iodobenzaldehyde (**4**) with (trimethylsilyl)-acetylene under Pd-mediated coupling conditions (35 °C for 48 h under argon)[24] gave **5** in 75% yield after Kugelrohr distillation (Scheme 1). The unwanted enyne product, present at ∼3% as evidenced by GC-MS, was readily removed by column chromatography on silica.

**Scheme 1.** Aldehyde Precursors for Preparing the Porphyrins[a]

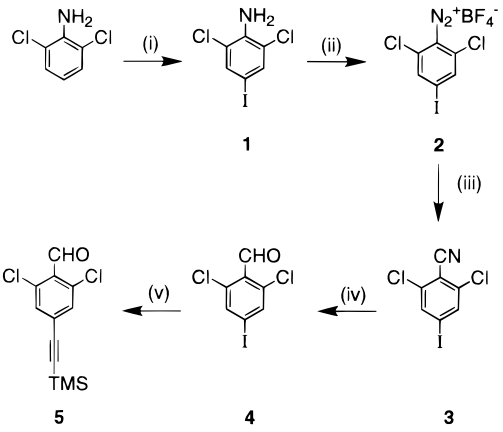


[a] Reagents and conditions: (i) Benzyltrimethylammonium dichloroiodate in $MeOH/CH_2Cl_2$, Δ, 2 h; (ii) $H_2SO_4/H_2O$, $NaNO_2$, $NaBF_4$, 0 °C; (iii) CuCN/NaCN, $H_2O$; (iv) DIBAL-H, $CH_2Cl_2$, 0 °C, $HCl/H_2O$; (v) (trimethylsilyl)acetylene, $Pd_2(dba)_3$, $AsPh_3$, toluene/$Et_3N$, 35 °C.

**2. $A_3B$ Porphyrin Building Blocks.** Porphyrin building blocks bearing a functional group (iodo, ethyne) at one of the four meso positions provide the basis for constructing the dimeric arrays. These $A_3B$ porphyrin building blocks can be obtained through mixed aldehyde−pyrrole condensations using the two-step one-flask room-temperature synthesis[21,22] (Scheme 2). The method of mixed aldehyde−pyrrole condensations affords a mixture of six porphyrins. The separability of mixtures of porphyrins by adsorption chromatography depends on the facial encumbrance due to ortho substituents and on the different polarity of all of the aryl substituents.[20] For mixtures that are difficult to separate, metalation of the mixture of Fb porphyrins affords the Zn porphyrins, which often can be easily separated via column chromatography.[8,14] The introduction of zinc imparts a polar site which enhances the affinity of the porphyrins for silica gel and accentuates effects of facial encumbrance. Thus, for the preparation of ethyne-substituted porphyrins, crude aldehyde−pyrrole condensation mixtures were concentrated and passed over a flash silica column to remove reagents and byproducts. The porphyrin mixtures were treated with methanolic zinc acetate, and the resulting Zn porphyrins were

(18) Kirmaier, C.; Holten, D. *Biochemistry* **1991**, *30*, 609−613.
(19) Lindsey, J. S. In *Modular Chemistry*; Michl, J., Ed., NATO ASI Series C: Mathematical and Physical Sciences; Vol. 499, Dordrecht, 1997; Kluwer Academic Publishers: pp 517−528.
(20) Lindsey, J. S.; Prathapan, S.; Johnson, T. E.; Wagner, R. W. *Tetrahedron* **1994**, *50*, 8941−8968.
(21) Lindsey, J. S.; Wagner, R. W. *J. Org. Chem.* **1989**, *54*, 828−836.
(22) Lindsey, J. S.; Schreiman, I. C.; Hsu, H. C.; Kearney, P. C.; Marguerettaz, A. M. *J. Org. Chem.* **1987**, *52*, 827−836.
(23) Lamm, B.; Andersson, B. *Acta Chem. Scand.* **1969**, *23*, 3355−3360.
(24) Wagner, R. W.; Johnson, T. E.; Li, F.; Lindsey, J. S. *J. Org. Chem.* **1995**, *60*, 5266−5273.

**Scheme 2.** Separation of Porphyrin Building Blocks

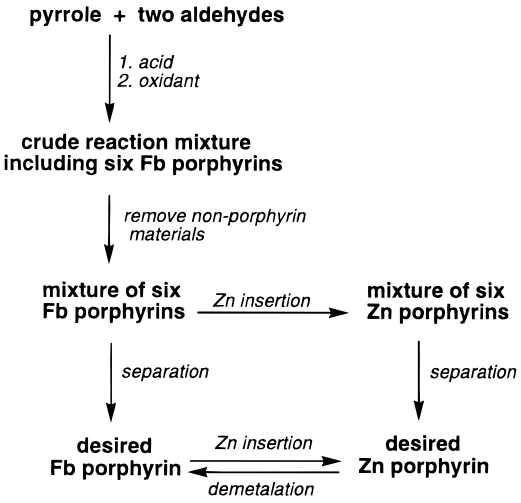


**Scheme 3.** Synthesis of Dimeric Arrays

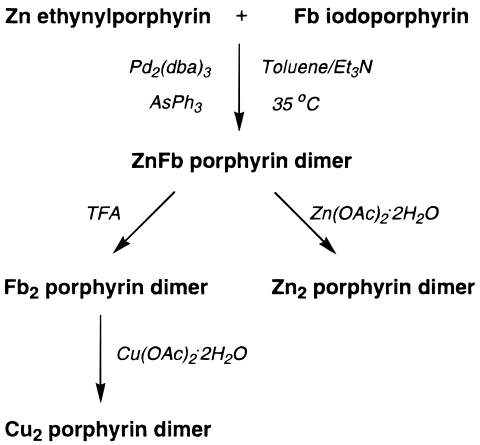


separated on a silica column to give the desired $A_3B$ porphyrin (Chart 2). The corresponding Fb porphyrins were prepared by demetalation. On the other hand, the desired Fb iodo porphyrin $FbIH(Cl_2)$ (Chart 2) could be separated from its mixture as the Fb porphyrin by column chromatography on silica without the need for metalation and demetalation. The Zn ethynyl porphyrin $ZnH(Cl_2)'$ was prepared by deprotecting the trimethylsilyl-protected porphyrin with tetrabutylammonium fluoride on silica.

**3. Dimeric Arrays.** The preparation of the dimeric arrays relies on Pd-mediated coupling reactions[24] of ethynylporphyrins and iodoporphyrins (Scheme 3). The reaction of the Fb iodoporphyrin $FbIH(Cl_2)$ and the Zn ethynylporphyrin $ZnH(Cl_2)'$ with $Pd_2(dba)_3$ and $AsPh_3$ in toluene/triethylamine (5:1) at 35 °C under argon for 2 h afforded the diphenylethyne-linked dimer $ZnFbB(Cl_4)$. The crude reaction mixture consisted of small amounts of higher molecular weight material (uncharacterized), desired $ZnFbB(Cl_4)$, monomeric porphyrins, and reagents. The progress of the reaction could be assessed by silica TLC or by analytical SEC. For preparative purification, a flash silica column with hexanes−$CH_2Cl_2$ (1:1) removed $AsPh_3$ and left the Pd residue on the top of the column. Passing the resultant mixture over a preparative SEC column in THF (twice) removed the unwanted higher molecular weight material and porphyrin monomers. The fraction containing the desired $ZnFbB(Cl_4)$ dimer was then passed over a silica column eluting with hexanes−$CH_2Cl_2$ (2:1). Fractions were assessed for purity by analytical SEC. This method afforded 67 mg of $ZnFbB(Cl_4)$ in 75% yield. This same approach with other porphyrin building blocks afforded the dimer $Fb_2B(CH_3)_4$ in comparable yield (Chart 2). In each case there were no detectable impurities (>99%) based on integrated peak area in the analytical SEC.

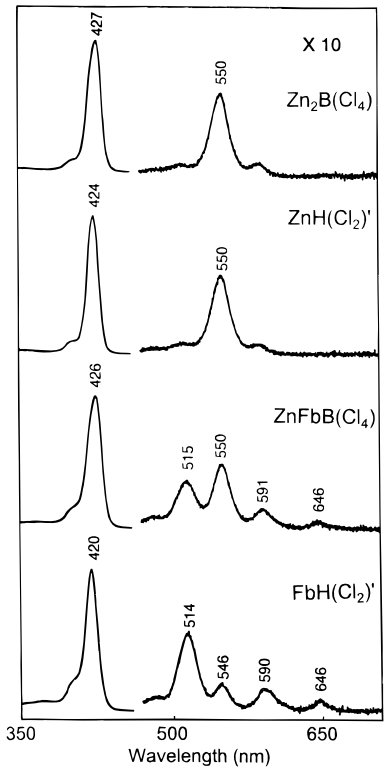


**Figure 1.** Absorption spectra in toluene at room temperature of the monomeric building blocks and the dimeric arrays.

The bis-Zn dimer $Zn_2B(Cl_4)$ was prepared in quantitative yield by treatment of the corresponding ZnFb dimer with methanolic zinc acetate. The zinc insertion was quantitative. The bis-Cu dimers ($Cu_2B(Cl_4)$, $Cu_2B(CH_3)_4$) were prepared by treating the corresponding $Fb_2$ dimers (obtained by direct synthesis or by demetalating the ZnFb dimers with trifluoroacetic acid) with methanolic cupric acetate (Scheme 3). These metal insertions also were quantitative. This building block approach provided ready access to small quantities of the various dimers.

**B. Physical Properties of the Neutral Complexes. 1. Absorption Spectra.** The absorption spectra of selected monomeric and dimeric chlorine-containing porphyrins are shown in Figure 1. The general spectral features of all the compounds (strong B- and weak Q-bands) are similar to those we have previously reported for other arrays and their building blocks.[2−9] The spectra of the dimers are approximately a superposition of the absorption spectra of the Zn and Fb porphyrin constituents, indicative of the relatively weak interactions between the porphyrins. The absorption spectra of the chlorine-containing arrays are very similar to those of their TPP analogues.

**2. Fluorescence Quantum Yields and Lifetimes.** The fluorescence yields and lifetimes of $ZnFbB(Cl_4)$, the non-chlorinated, hindered analogue $ZnFbB(CH_3)_4$, and a number of monomeric building blocks in toluene and DMSO are collected in Table 1. The fluorescence spectra of $ZnFbB(Cl_4)$ and the chlorine-containing monomers are very similar to those reported previously for the non-chlorinated complexes.[6,8,9] The emission from $ZnFbB(Cl_4)$ comes predominantly from the photoexcited Fb porphyrin (Fb*) independent of whether the Zn or Fb porphyrin is excited, as has been reported for $ZnFbB(CH_3)_4$ and

**Table 1.** Singlet Excited-State Lifetimes and Fluorescence Yields[a]

| | | Zn porphyrin | | Fb porphyrin | |
|---|---|---|---|---|---|
| porphyrin | solvent | $\tau$ (ns) | $\Phi_f$ | $\tau$ (ns) | $\Phi_f$ |
| dimers | | | | | |
| ZnFbB($Cl_4$) | toluene | 0.13 | <0.002 | 4.6 | 0.038 |
| | DMSO | 0.19[b] | | 4.0 | 0.033 |
| ZnFbB($CH_3$)$_4$ | toluene | 0.11, 0.090[c] | <0.005[c] | 12.9, 12.2[c] | 0.10[c] |
| | DMSO | 0.12, 0.085[c] | <0.006[c] | 10.1, 10.8[c] | 0.092[c] |
| monomers | | | | | |
| ZnH($Cl_2$) | toluene | 4.4 | 0.059 | | |
| ZnH($Cl_2$)′ | toluene | 4.3 | 0.050 | | |
| | DMSO | 3.4 | 0.053 | | |
| ZnH($CH_3$)$_2$ | toluene | 2.3[c] | 0.039[c] | | |
| ZnTPP | toluene | 2.2, 2.0[c] | 0.033[d] | | |
| FbH($Cl_2$)′ | toluene | | | 4.9 | 0.034 |
| | DMSO | | | 4.1 | 0.037 |
| FbH($CH_3$)$_2$ | toluene | | | 12.7[c] | 0.11[c] |
| TPP | toluene | | | 13.2, 11.5[c] | 0.11[d] |

[a] Data were collected at ~295 K. The excited-state lifetimes were determined by time-resolved fluorescence (±5%) in degassed solutions, except for lifetimes of the excited Zn porphyrins in the dimers, which were measured using transient absorption spectroscopy (±10%). The Zn* lifetimes reported from the transient absorption studies are derived from dual exponential fits to the data (see Figure 2), with the longer component fixed at the Fb* lifetime determined via fluorescence decay. [b] For ZnFbB($Cl_4$) in DMSO, the time constant obtained in the Soret-region transient absorption (450−490 nm) is somewhat longer (270 ps) than that obtained in the 500−550-nm region of the Q-band bleachings (115 ps). An average of the time constants determined in the two regions is reported for each sample. Further studies in other polar solvents are required to ascertain the origin of this wavelength dependence, which could derive from inhomogeneities associated with differing states of metal ligation in DMSO. [c] Reference 6. Note that the fluorescence yields of the Zn porphyrins were scaled from those in that paper by a factor of 0.033/0.030 to account for a revised value (see footnote *d*) of the fluorescence yield of the ZnTPP standard. [d] The yield of 0.033 for ZnTPP was used as the reference for the Zn porphyrins, and the yield of 0.11 for TPP was used as the reference for the Fb porphyrins.[38,39]

a number of other ZnFb arrays.[6,8,9] This observation is indicative of fast and highly efficient energy transfer from the photoexcited Zn porphyrin (Zn*) to the Fb porphyrin, a process that is quantitated from the time-resolved absorption data (vide infra).

Although this study focuses on the energy-transfer process from Zn* to the Fb porphyrin in ZnFbB($Cl_4$) relative to that in ZnFbB($CH_3$)$_4$, we also examined the photophysical properties of Fb* in the dimers and their building blocks, as well as the Zn* lifetime in the building blocks (Table 1). The primary findings are as follows: (1) The Fb* lifetime and fluorescence yield of ZnFbB($Cl_4$) are reduced by about 60% from the values for ZnFbB($CH_3$)$_4$. The Fb* lifetimes and emission yields of both dimers are comparable to those of the corresponding monomeric building blocks. These results, together with the static absorption and emission spectra, indicate that the reduced Fb* lifetimes and emission yields in ZnFbB($Cl_4$) versus those for ZnFbB($CH_3$)$_4$ result from enhanced nonradiative decay of Fb* rather than from a change in the natural radiative rate. (2) The lifetimes of Fb* in the monomers and dimers are similar to one another both in toluene and in the polar solvent DMSO, indicating that charge-transfer quenching of Fb* by the Zn porphyrin in ZnFbB($Cl_4$) is not appreciable (<10%), as has also been observed for ZnFbB($CH_3$)$_4$.[6] (3) The Zn* lifetimes and fluorescence yields of ZnH($Cl_2$)′ and ZnH($Cl_2$) are *increased* almost 2-fold relative to ZnH($CH_3$)$_2$ and ZnTPP. Thus, the presence of one 2,6-dichloroaryl group has multiple opposing effects on excited-state lifetimes and yields. The interplay of these factors, which offer the prospect of fine-tuning the properties of photonic devices, has been explored in a set of 40 Fb porphyrins and metalloporphyrins containing differing numbers of various halogenated aryl units.[25]

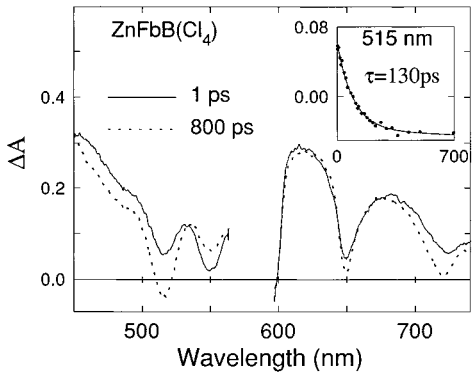


**Figure 2.** Transient difference spectra acquired following excitation of ZnFbB($Cl_4$) in toluene at room temperature with a 0.2-ps flash at 582 nm. The spectra for the array was acquired with time delays of 1 ps (solid traces) or 800 ps (dashed traces). Note that the data in the red region were acquired with a sample concentration ~10-fold greater than that used for the blue region. Consequently, a quantitative comparison of the absorption changes in the two regions should not be made. The inset shows a representative kinetic trace at 515 nm with a fit to a dual exponential which takes into account both the fast decay of Zn* and the slow decay of Fb*. The Fb* lifetime was fixed at the value of 4.6 ns obtained from the fluorescence lifetime measurements (Table 1).

**3. Time-Resolved Absorption Spectra.** The energy-transfer rate from Zn* to Fb in ZnFbB($Cl_4$) was probed using ultrafast absorption difference spectroscopy. Representative data are shown in Figure 2. The 582-nm excitation flashes excite both Zn and Fb porphyrins. Therefore, the absorption difference spectra acquired shortly after excitation contain features characteristic of Zn* in those arrays in which the Zn porphyrin was excited and features characteristic of Fb* in those arrays in which the Fb porphyrin was excited.

Assignments of the spectra shown in Figure 2 were made by direct analogy with the those previously described for other Zn porphyrin arrays such as ZnFbB($CH_3$)$_4$ and the unhindered parent dimer ZnFbU.[6,8,9] In particular, between 1 and 800 ps there is simultaneous decay of the Zn porphyrin bleaching at 550 nm, increased Fb porphyrin bleaching at 515 nm, and increased Fb* stimulated emission at 715 nm. These changes reflect simultaneous decay of Zn* and formation of Fb* in the fraction of dimers in which the Zn porphyrin was originally excited. The results demonstrate that energy transfer, Zn*Fb → ZnFb*, is the primary mode of Zn* decay in these arrays (vide infra). The absorption difference spectra observed following complete decay of Zn* (e.g., 800-ps spectrum) can be assigned to Fb*.

The insets in Figure 2 show representative kinetic data and a fit giving a time constant of 130 ± 15 ps for the Zn* lifetime of ZnFbB($Cl_4$) in toluene. The same time constant is obtained in other regions of the spectrum where there are sufficiently large changes in $\Delta A$ as a function of time. Subsequent decay of Fb* occurs with a time constant of 4.6 ns for ZnFbB($Cl_4$) in toluene, as determined via the fluorescence decay profiles (vide supra). Similar results are obtained in DMSO (Table 1).

**4. The Rates, Yields, and Mechanism of Energy Transfer.** The intrinsic rate constant ($k_{trans}$) and quantum yield ($\Phi_{trans}$) for the Zn*Fb → ZnFb* energy-transfer process were obtained from

(25) Yang, S. I.; Seth, J.; Strachan, J. P.; Gentemann, S.; Kim, D.; Holten, D.; Lindsey, J. S.; Bocian, D. F. *J. Phys. Chem.* submitted for publications.

the kinetic data using the following relationships:

$$k_{trans} = (\tau_{Zn^*})^{-1} - (\tau^{\circ}_{Zn^*})^{-1} \quad (1)$$

$$\Phi_{trans} = k_{trans}\,\tau_{Zn^*} = 1 - \tau_{Zn^*}/\tau^{\circ}_{Zn^*} \quad (2)$$

Here, $\tau_{Zn^*}$ is the measured lifetime of the excited Zn porphyrin and $\tau^{\circ}_{Zn^*}$ is the Zn* lifetime of the relevant monomer in toluene (Table 1). This analysis assumes that the dramatic reduction in the Zn* lifetime in the dimer exclusively reflects energy transfer to the Fb porphyrin. In particular, it assumes that the inherent rate constants for the fluorescence, internal conversion, and intersystem crossing decay pathways of Zn* have the same values in the dimer as in the corresponding monomer, and that charge-transfer quenching of Zn* by the Fb porphyrin makes a minimal (<10%) contribution to the photodynamics in toluene. The latter is evidenced by the data given above for ZnFbB-($Cl_4$) and previously for a number of other ZnFb dimers.[6,8,9]

Using eqs 1 and 2 and the measured lifetimes in Table 1, the rate and yield of energy transfer from Zn* to the Fb porphyrin in ZnFbB($Cl_4$) are calculated to be $k_{trans} = (134\ ps)^{-1}$ and $\Phi_{trans} = 97\%$. Energy transfer to the Fb porphyrin dominates the decay of Zn*. This fact is evident from the observation that the calculated energy-transfer rate constant is nearly equal to the observed excited-state decay rate of $(130\ ps)^{-1}$. The energy-transfer rate and yield for ZnFbB($Cl_4$) are comparable to that of the torsionally constrained dimer ZnFbB($CH_3$)$_4$ ($k_{trans} = (115\ ps)^{-1}$, $\Phi_{trans} = 95\%$) but differ significantly from the values for the unconstrained dimer ZnFbU ($k_{trans} = (24\ ps)^{-1}$, $\Phi_{trans} = 99\%$).

The finding of comparable energy-transfer rates in ZnFbB-($Cl_4$) and ZnFbB($CH_3$)$_4$ argues that the attenuation in electronic communication in these dimers relative to ZnFbU stems from steric constraints imposed by the *o*-chloro or *o*-methyl groups of the linker. The ortho substituents impede rotation of the linker aryl groups with respect to the porphyrin macrocycles, as we have previously discussed for ZnFbB($CH_3$)$_4$.[6] Hindered rotation increases the average torsional angle between the linker and the porphyrin, thereby diminishing orbital overlap. This effect dominates other effects of the *o*-chloro substituents, such as electron withdrawal and interaction of the p orbitals of the *o*-chloro substituents with the p orbitals of the *meso*-carbon[11] (vide infra).

The realization that steric constraints on electronic communication in ZnFbB($Cl_4$) (as in ZnFbB($CH_3$)$_4$) underlie the reduced rate and efficiency of energy transfer relative to those observed for the unhindered analogue ZnFbU has important consequences. In particular, it provides additional experimental support for the contention that the predominant mechanism for energy transfer in the diphenylethyne-linked porphyrin arrays is through-bond (TB) rather than through-space (TS) in nature.[6] Indeed, calculations based on the Förster TS mechanism[26] indicate that the various dimers (ZnFbB($Cl_4$), ZnFbB($CH_3$)$_4$, and ZnFbU) have TS rates ($k_{TS}$) that differ by less than a factor of 2 (Table 3), far smaller than the experimentally observed 5-fold difference in energy-transfer rates in the torsionally constrained versus unconstrained arrays. The Förster TS rate for ZnFbB-($Cl_4$) is calculated to be $(1.071\ ns)^{-1}$, in contrast to the much faster observed rate of $(0.134\ ns)^{-1}$. The Förster analysis assumes that each of the dimers has the same value for the orientation term of the transition dipoles of the Zn and Fb porphyrins ($\kappa^2 = 1.125$).[6] However, any differences in orientation factor that might occur due to the presence of linker substituents are insufficient to account for the differences in energy-transfer rates of the various dimers.

(26) Lamola, A. A. In *Energy Transfer and Organic Photochemistry*; Lamola, A. A., and Turro, N. J., Eds.; Interscience: New York 1969.

**Table 2.** Half-Wave Potentials[a] for Oxidation of the Porphyrins of the Various Arrays

| | Zn porphyrin | | Fb porphyrin | |
|---|---|---|---|---|
| | $E_{1/2}$ (**1**) | $E_{1/2}$ (**2**) | $E_{1/2}$ (**1**) | $E_{1/2}$ (**2**) |
| FbH($Cl_2$)′ | | | 0.83 | 1.19 |
| ZnH($Cl_2$)′ | 0.68 | 1.00 | | |
| ZnFbB($Cl_4$) | 0.68 | 1.00 | 0.83 | 1.19 |
| $Zn_2$B($Cl_4$)[b] | 0.68 | 1.00 | | |

[a] Obtained in $CH_2Cl_2$ containing 0.1 M TBAH. $E_{1/2}$ vs $Ag/Ag^+$; $E_{1/2}$ of $FeCp_2/FeCp_2^+ = 0.22$ V; scan rate = 0.1 V/s. Values are ±0.01 V. [b] The redox waves of the two Zn porphyrins are not resolved by cyclic voltammetry.

The dominance of the TB mechanism for ZnFbB($Cl_4$) (and the other arrays) can be seen by assuming that the observed energy-transfer rate ($k_{trans}$) is determined by the additive effects of TB and TS processes (eq 3).[6,8,9] The fractional amounts of the TB ($\chi_{TB}$) and TS ($\chi_{TS}$) contributions can then be estimated (eqs 4 and 5). The resulting TB energy-transfer rate for ZnFbB-

$$k_{trans} = k_{TB} + k_{TS} \quad (3)$$

$$\chi_{TB} = k_{TB}/k_{trans} \quad (4)$$

$$\chi_{TB} + \chi_{TS} = 1 \quad (5)$$

($Cl_4$) is $(153\ ps)^{-1}$, and this pathway accounts for ~88% of the total energy transfer. A similarly high percentage is found for the other dimers (Table 3). Consequently, the TB rate in ZnFbB($Cl_4$) is nearly identical to that in its sterically similar counterpart ZnFbB($CH_3$)$_4$ ($(140\ ps)^{-1}$) but is about 5-fold slower than in the unhindered parent complex ZnFbU ($(25\ ps)^{-1}$). Again, these comparisons reflect (1) the similar steric constraints imposed by *o*-chloro and -methyl groups incorporated into the diphenylethyne linker on electronic communication and (2) the dominance of the sterically mediated electronic effect in ZnFbB-($Cl_4$) over other potential effects of the *o*-chloro substituents.

**5. RR Spectra.** The high-frequency regions of the B-state excitation ($\lambda_{exc}$ = 457.9 nm) RR spectra of ZnFbB($Cl_4$) and $Zn_2$B($Cl_4$) are shown in Figure 3. The scattering characteristics of the porphyrin skeletal modes of the chlorine-containing arrays are similar to those observed for other arylethyne-linked arrays and are generally unremarkable.[5,7] The key spectral feature shown in the figure is the ethyne stretching mode, $\nu_{C\equiv C}$,[5,7] which is observed at ~2215 $cm^{-1}$. The RR intensities of the $\nu_{C\equiv C}$ modes of ZnFbB($Cl_4$) and $Zn_2$B($Cl_4$) are modest compared with those of the porphyrin skeletal modes. However, the RR intensities of the $\nu_{C\equiv C}$ modes (compared with the porphyrin modes) of the chlorine-containing dimers are somewhat larger (~3-fold) than those reported previously[6] for the analogous modes of ZnFbB($CH_3$)$_4$ and $Zn_2$B($CH_3$)$_4$. The increased RR intensities observed for the $\nu_{C\equiv C}$ modes of the two different classes of torsionally constrained dimers indicate that the B-excited-state electronic coupling between the ethyne group and the $\pi$ system of the porphyrin ring (which dictates the relative RR intensities of the $\nu_{C\equiv C}$ versus porphyrin skeletal modes[5,7]) is somewhat larger for the chlorine-containing arrays.

Although the linker-mediated electronic coupling in the B-excited state is interesting in its own right, the energy transfer involves the Q-excited states. However, as is the case for other ZnFb and bis-Zn porphyrins, Q-state excitation RR spectra cannot be obtained for the chlorine-containing dimers owing

**Table 3.** Through-Bond (TB) vs Through-Space (TS) Energy-Transfer Rates and Efficiencies for Various ZnFb Dimers[a]

| porphyrin | $\epsilon_{510}$[b] | $\epsilon_{550}$[b] | $\Phi_f$[c] | $\tau$ (ns)[c] | $J$ (cm$^6$ mmol$^{-1}$)[d] | $k_{trans}^{-1}$ (ps) | $\Phi_{trans}$[e] | $k_{TS}^{-1}$ (ps) | $k_{TB}^{-1}$ (ps) | $\chi_{TB}$ | $\chi_{TS}$ |
|---|---|---|---|---|---|---|---|---|---|---|---|
| ZnFbU | 19000 | 7800 | 0.035 | 2.38 | $2.94 \times 10^{-14}$ | 24 | 0.99 | 745 | 25 | 0.96 | 0.04 |
| ZnFbB($CH_3$)$_4$ | 22000 | 8900 | 0.032 | 2.26 | $3.53 \times 10^{-14}$ | 115 | 0.95 | 644 | 140 | 0.82 | 0.18 |
| ZnFbB($Cl_4$) | 19500 | 7750 | 0.050 | 4.4 | $2.65 \times 10^{-14}$ | 134 | 0.97 | 1071 | 153 | 0.88 | 0.12 |

[a] All data were obtained in toluene at room temperature. [b] Peak extinction coefficients in $M^{-1}$ cm$^{-1}$. [c] For the Zn porphyrin in the absence of a Fb porphyrin. [d] The Förster spectral overlap term is computed using selected monomers which best approximate those units in the dimer. The spectral overlaps are generally in accord with those obtained for other porphyrin systems.[2,6,40] [e] Calculated from eq 4.

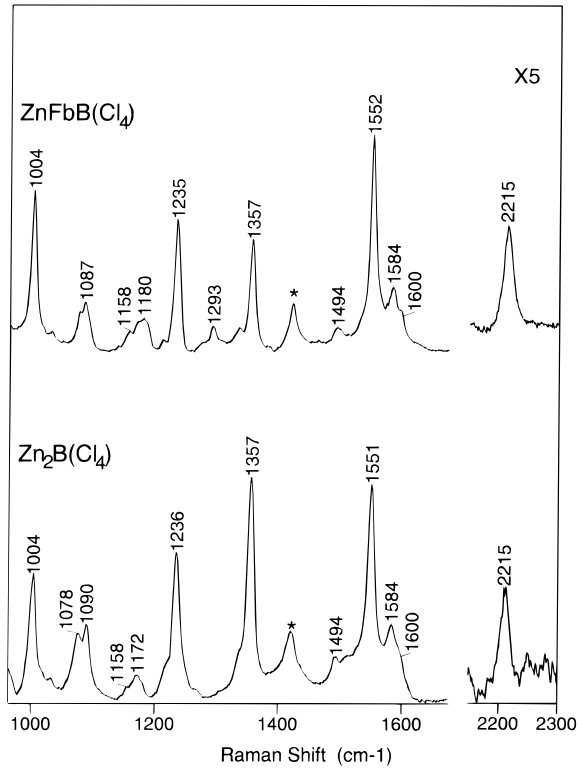


**Figure 3.** High-frequency regions of the B-state excitation ($\lambda_{exc}$ = 457.9 nm) RR spectra of ZnFbB($Cl_4$) and $Zn_2B(Cl_4)$ at room temperature. The bands marked by asterisks are due to solvent.

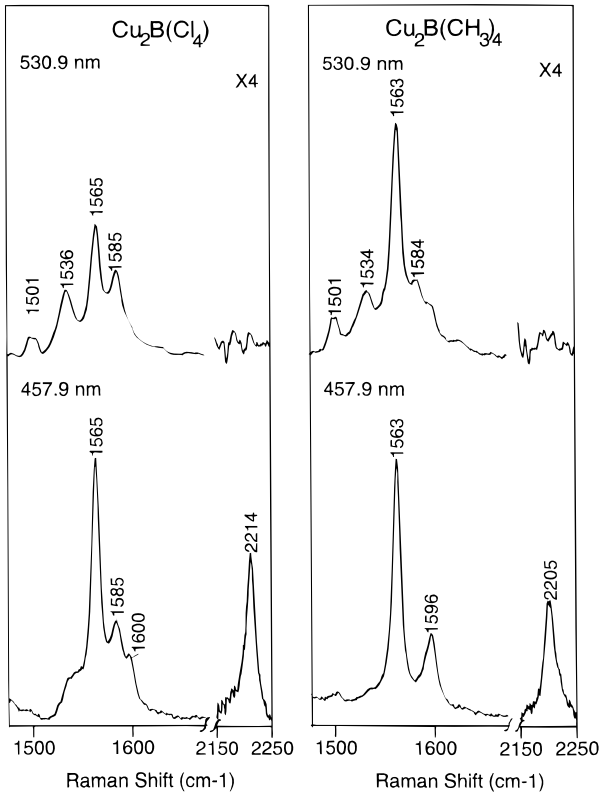


**Figure 4.** RR spectra of $Cu_2B(Cl_4)$ (left panel) and $Cu_2B(CH_3)_4$ (right panel) obtained with B-state ($\lambda_{exc}$ = 457.9 nm) and Q-state ($\lambda_{exc}$ = 530.9 nm) excitation at room temperature.

to interference from fluorescence.[5,9] Therefore, complete sets of RR spectra (B- and Q-state excitation) were instead acquired for the bis-Cu complexes of the chlorine-containing dimers, which exhibit little or no emission in the Q-state region. In order to make a more direct comparison with the RR spectra of $Cu_2B(Cl_4)$, B- and Q-state excitation RR spectra were also obtained for the Cu(II) analogue of the bis-hindered array we have previously studied,[7] $Cu_2B(CH_3)_4$.

Figure 4 shows the high-frequency regions of the RR spectra of $Cu_2B(Cl_4)$ (left panel) and $Cu_2B(CH_3)_4$ (right panel) obtained with B- and Q-state excitation. The absolute RR intensities observed at the different excitation wavelengths cannot be compared directly because the sample concentrations required to obtain reasonable quality Q-state spectra are higher than those necessary for B-state studies. The RR data obtained for both $Cu_2B(Cl_4)$ and $Cu_2B(CH_3)_4$ show that the $\nu_{C\equiv C}$ mode exhibits appreciable RR intensity with excitation in the B-state region (457.9 nm). This behavior parallels that observed for the chlorine-containing bis-Zn and ZnFb arrays (Figure 3). In contrast, both $Cu_2B(Cl_4)$ and $Cu_2B(CH_3)_4$ exhibit little enhancement of the $\nu_{C\equiv C}$ mode with excitation resonant with the Q-state absorption. The minimal (or negligible) RR enhancement observed for the $\nu_{C\equiv C}$ modes of $Cu_2B(Cl_4)$ and $Cu_2B(CH_3)_4$ indicates that the Q-excited-state electronic coupling between the ethyne group and the $\pi$ system of the porphyrin is weak for both of these bis-hindered arrays. Much stronger porphyrin-ethyne Q-excited-state electronic coupling is observed for the unhindered dimer $Cu_2U$, as is indicated by the significant enhancement of its $\nu_{C\equiv C}$ mode.[9] These observations are in accord with the relatively slow energy-transfer rates observed for both ZnFbB($Cl_4$) and ZnFbB($CH_3$)$_4$ relative to that of ZnFbU (vide infra).

**C. Physical Properties of the Oxidized Complexes.** The oxidized arrays were investigated to gain insight into how the incorporation of *o*-chloro substituents on the linker modulates the rates of hole/electron hopping.[5,7] These rates are of interest because no independent assessment of the rates of charge transfer is available for the neutral arrays. Although the hole/electron-hopping rates in the ground electronic states of the cations are not expected to be equal to the charge-transfer rates in the excited states of the neutrals, they at least provide some measure of the factors which control this type of process.

**1. Electrochemistry.** The $E_{1/2}$ values for oxidation of the chlorine-containing dimeric arrays and the monomeric building blocks are summarized in Table 2. The two $E_{1/2}$ values listed in the table correspond to the first and second oxidations of the porphyrin ring.[27] The redox characteristics of the chlorine-

(27) (a) Felton, R. H. In *The Porphyrins*; Dolphin, D., Ed.; Academic Press: New York, 1978; Vol. V, pp 53−126. (b) Davis, D. G. *Ibid*.; pp 127−152.

containing arrays closely resemble those of other arylethyne-linked arrays we have previously investigated.[5,7] The potentials are positively shifted relative to the non-chlorinated analogues; however, this shift is relatively small (~0.06 V) and commensurate with the small number of modestly electron-withdrawing chloro substituents.[28] In particular, for $ZnFbB(Cl_4)$, four overlapping redox waves are observed, two each for the Zn and Fb porphyrins. For $Zn_2B(Cl_4)$, two redox waves are observed whose peak-to-peak separations are ~70 mV. Quantitative coulometry confirms that each wave corresponds to the removal of two electrons. Differential pulse and square-wave voltammetry on the $Zn_2B(Cl_4)$ fails to resolve peaks due to the individual one-electron oxidations; however, the peaks exhibit asymmetries which indicate small inequivalences between the redox potentials of the individual Zn porphyrins (50 mV or less).

As observed for non-chlorinated arylethyne-substituted porphyrins,[5,7] the chlorine-containing arylethyne-substituted porphyrins do not exhibit any redox characteristics which would suggest that there is any significant ground-state interaction between the porphyrin and arylethyne group $\pi$ systems. Indeed, such porphyrin−arylethyne group interaction is not anticipated because the $E_{1/2}$ value for oxidation of diphenylethyne is 1.64 V versus SCE[29] and its absorption $\lambda_{max}$ occurs at ~300 nm,[30] indicating that the highest occupied and lowest unoccupied molecular orbitals of diphenylethyne span those of the porphyrins. The presence of four *o*-chloro substituents on the diarylethyne group would tend to lower its potential and red-shift its $\lambda_{max}$; however, these effects are necessarily quite small considering that the redox and optical characteristics of the chloro-substituted porphyrin monomers and dimers are very similar to those of the non-chlorine-containing analogues.[5,7] Collectively, the redox characteristics of $ZnFbB(Cl_4)$ and $Zn_2B(Cl_4)$ are indicative of relatively small ground-state electronic interaction between the porphyrin constituents.

**2. Absorption Spectra.** The UV−vis absorption characteristics of the mono- and dications of the arrays (not shown) are typical of those of other porphyrin $\pi$-cation radicals, namely weaker, blue-shifted B bands (relative to the neutral complexes) and very weak, broad bands in the visible and near-infrared regions.[27a] The absorption spectra of the oxidized complexes appear to be a superposition of the spectra of the neutral and cationic species of the different porphyrin units. This observation, like the results of the electrochemical studies,[31−34] is consistent with weak interactions between the constituent porphyrins.

**3. EPR Spectra.** The EPR spectra of the oxidation products of $ZnH(Cl_2)'$ and $Zn_2B(Cl_4)$ are shown in Figure 5. The EPR spectra of all of the cations were examined as a function of sample concentration. No changes in hyperfine splittings or line shape were observed for the concentrations used for the EPR studies (≤0.05 mM). Consequently, the differences observed in the spectral features of the various complexes are intrinsic and cannot be ascribed to intermolecular interactions.

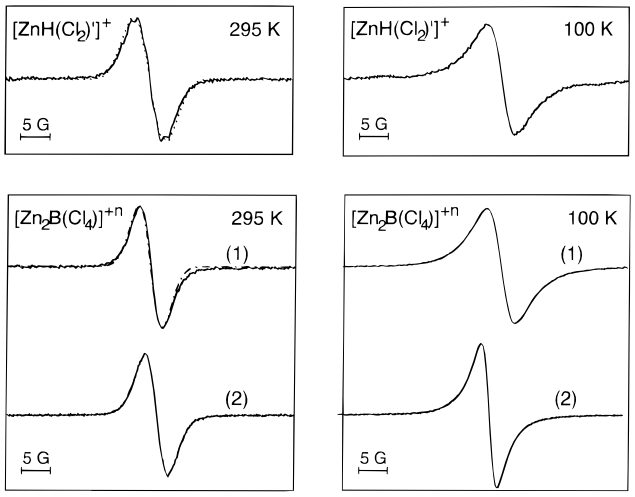


**Figure 5.** EPR spectra of $[ZnH(Cl_2)']^+$ and $[Zn_2B(Cl_4)]^{+n}$ ($n = 1, 2$) obtained at 295 and 100 K (solid lines). The additional traces shown for $[ZnH(Cl_2)']^+$ and $[Zn_2B(Cl_4)]^+$ at 295 K are simulated spectra. For $[ZnH(Cl_2)']^+$, the simulated spectrum was obtained with the following parameters: $a(^{14}N) = 1.39$ G, $a(^1H_{o-aryl}) = 0.36$ G, Lorentzian fwhm = 1.25 G. For $[Zn_2B(Cl_4)]^+$, the simulated spectrum was obtained by reducing the hyperfine splittings by a factor of 2, doubling the number of interacting nuclei, and holding the line width constant.

The liquid-solution EPR spectrum of $[ZnH(Cl_2)']^+$ exhibits a poorly resolved nine-line hyperfine pattern due to interaction of the unpaired electron with the four pyrrole $^{14}N$ nuclei (Figure 5). This spectral pattern is characteristic of a $^2A_{2u}$ porphyrin $\pi$-cation radical.[35] This ground electronic state is expected for the cation radical of a porphyrin containing a single 2,6-dichloroaryl group. This is so because porphyrins containing four 2,6-dichlorophenyl groups still exhibit a ground electronic state which is predominantly $^2A_{2u}$ in character.[11,36,37] Simulations of the EPR spectrum of $[ZnH(Cl_2)']^+$ (Figure 5, top left panel) indicate that the $^{14}N$ hyperfine splittings ($a(^{14}N) \sim 1.39$ G) are generally comparable to, but slightly smaller than, those measured for $[ZnTPP]^+$ or any other Zn porphyrin monomer radical cations of this family ($a(^{14}N) \sim 1.45-1.65$ G).[5,7,35] The relatively small reduction in the $^{14}N$ splitting relative to that of non-chlorine-containing porphyrins is commensurate with the modest electron-withdrawing capabilities afforded by the single 2,6-dichloroaryl group on the porphyrin (vide supra). In frozen solution, no hyperfine structure is resolved for $[ZnH(Cl_2)']^+$;

(28) Ghosh, A. *J. Am. Chem. Soc.* **1995**, *117*, 4691−4699.
(29) Cariou, M.; Simonet, J. *J. Chem. Soc., Chem. Commun.* **1990**, 445−446.
(30) Armitage, J. B.; Entwistle, N.; Jones, E. R. H.; Whiting, M. C. *J. Chem. Soc.* **1954**, 147−154.
(31) Heath, G. A.; Yellowlees, L. J.; Braterman, P. S. *J. Chem. Soc., Chem. Commun.* **1981**, 287−289.
(32) Elliot, C. M.; Hershenhart, E. *J. Am. Chem. Soc.* **1982**, *104*, 7519−7526.
(33) Edwards, W. D.; Zerner, M. C. *Can. J. Chem.* **1985**, *63*, 1763−1772.
(34) (a) Angel, S. M.; DeArmond, M. K.; Donohoe, R. J.; Wertz, D. W. *J. Phys. Chem.* **1985**, *89*, 282−285. (b) Donohoe, R. J.; Tait, C. D.; DeArmond, M. K.; Wertz, D. W. *Spectrochim. Acta* **1986**, *42A*, 233−240. (c) Tait, C. D.; MacQueen, D. B.; Donohoe, R. J.; DeArmond, M. K.; Hanck, K. W.; Wertz, D. W. *J. Phys. Chem.* **1986**, *90*, 1766−1771. (d) Donohoe, R. R.; Tait, C. D.; DeArmond, M. K.; Wertz, D. W. *J. Phys. Chem.* **1986**, *90*, 3923−3926. (e) Donohoe, R. J.; Tait, C. D.; DeArmond, M. K.; Wertz, D. W. *J. Phys. Chem.* **1986**, *90*, 3927−3930.
(35) Fajer, J.; Davis, M. S. In *The Porphyrins*; Dolphin, D., Ed.; Academic Press: New York, 1979; Vol. IV, pp 197−256.
(36) (a) Fujii, H. *J. Am. Chem. Soc.* **1993**, *115*, 4641−4648. (b) Fujii, H.; Yoshimura, T.; Kamada, H. *Inorg. Chem.* **1996**, *35*, 2373−2377.
(37) Jayaraj, K.; Terner, J.; Gold, A.; Roberts, D. A.; Austin, R. N.; Mandon, D.; Weiss, R.; Bill, E.; Müther, M.; Trautwein, A. X. *Inorg. Chem.* **1996**, *35*, 1632−1640.
(38) Gouterman, M. In *The Porphyrins*; Dolphin, D., Ed.; Academic Press: New York, 1978; Vol. III, pp 1−165.
(39) Seybold, P. G.; Gouterman, M. *J. Mol. Spectrosc.* **1969**, *31*, 1−13.
(40) (a) Anton, J. A.; Loach, P. A.; Govindjee. *Photochem. Photobiol.* **1978**, *28*, 235−242. (b) Brookfield, R. L.; Ellul, H.; Harriman, A.; Porter, G. *J. Chem. Soc., Faraday Trans. 2* **1986**, *82*, 219−233. (c) Osuka, A.; Maruyama, K.; Yamazaki, I.; Tamai, N. *Chem. Phys. Lett.* **1990**, *165*, 392−396. (d) Gust, D.; Moore, T. A.; Moore, A. L.; Gao, F.; Luttrull, D.; DeGraziano, J. M.; Ma, X. C.; Makings, L. R.; Lee, S.-J.; Trier, T. T.; Bittersmann, E.; Seely, G. R.; Woodward, S.; Bensasson, R. V.; Rougée, M.; De Schryver, F. C.; Van der Auweraer, M. *J. Am. Chem. Soc.* **1991**, *113*, 3638−3649. (e) Sessler, J. L.; Wang, B.; Harriman, A. *J. Am. Chem. Soc.* **1995**, *117*, 704−714.

however, the peak-to-peak line width of the unresolved signal (∼5.3 G) is similar to the full width of the structured signal observed at room temperature.

The liquid and frozen solution EPR signatures observed for $[Zn_2B(Cl_4)]^+$ and $[Zn_2B(Cl_4)]^{+2}$ are generally similar to those previously reported for $[Zn_2B(CH_3)_4]^+$ and $[Zn_2B(CH_3)_4]^{+2}$.[5,7] In particular, the liquid solution EPR signals of both $[Zn_2B(Cl_4)]^+$ and $[Zn_2B(Cl_4)]^{+2}$ are much narrower (∼3.8 and ∼4.1 G, respectively) than that of $[ZnH(Cl_2)']^+$ (∼5.4 G) and do not exhibit any hyperfine structure. Upon freezing the solution, the EPR signal of $[Zn_2B(Cl_4)]^+$ broadens (∼5.3 vs ∼3.8 G) and becomes comparable in width to that of $[ZnH(Cl_2)']^+$ (∼5.3 G), whereas the signal of $[Zn_2B(Cl_4)]^{+2}$ exhibits additional narrowing (∼3.0 vs ∼4.1 G). The spectral signatures observed for $[Zn_2B(Cl_4)]^+$ and $[Zn_2B(Cl_4)]^{+2}$ indicate that the nature and rates of the hole/electron-hopping and exchange processes which are operative in the cations of these chlorine-containing arrays are qualitatively similar to those operative in $[Zn_2B(CH_3)_4]^+$ and $[Zn_2B(CH_3)_4]^{+2}$. In this connection, the liquid solution EPR spectrum of $[Zn_2B(Cl_4)]^+$ is well accounted for by halving the hyperfine coupling present in the monomer and doubling the number of interacting nuclei (while holding the line width constant) (Figure 5, bottom left panel). This result indicates that the hole/electron in $[Zn_2B(Cl_4)]^+$ is delocalized on the EPR time scale. The same conclusion has been drawn for $[Zn_2B(CH_3)_4]^+$ and $[Zn_2U]^+$.[6]

## Conclusions

The combined static and time-resolved spectroscopic and electrochemical investigations reported herein indicate that the incorporation of *o*-chloro groups on the diphenylethyne linker of ZnFb and bis-Zn dimers has significant steric, but not electronic, effects on both ground- and excited-state electronic communication. The magnitude of the effect of *o*-chloro group incorporation is comparable to that observed for *o*-methyl group incorporation. Other effects of the chloro groups, such as electron withdrawal and overlap with the $\pi$ orbitals of the porphyrin at the *meso*-carbons, are of little consequence. The results on the chlorinated dimers provide additional evidence that energy transfer in the diarylethyne-linked dimers predominantly occurs via a through-bond electron-exchange-mediated mechanism. The electron-withdrawing effect of the *o*-chloro groups enhances the robustness of the arrays by diminishing oxidative lability. These factors and the protocols developed to prepare and purify the complexes studied herein should find utility in the synthesis of the next generation of multiporphyrin arrays.

**Acknowledgment.** This work was supported by the Division of Chemical Sciences, Office of Basic Energy Sciences, Office of Energy Research, U.S. Department of Energy (J.S.L.), the LACOR Program (D.F.B.) from Los Alamos National Laboratory, and Grants GM36243 (D.F.B.) and GM34685 (D.H.) from the National Institute of General Medical Sciences. Mass spectra were obtained at the Mass Spectrometry Laboratory for Biotechnology at North Carolina State University. Partial funding for the facility was obtained from the North Carolina Biotechnology Center and the NSF.

IC970967C